Particle-laden jets: particle distribution and back-reaction on the flow



2011 J. Phys.: Conf. Ser. 318 052018

(http://iopscience.iop.org/1742-6596/318/5/052018)

# Particle-laden jets: particle distribution and back-reaction on the flow

**F. Picano[1], G. Sardina[1,2], P. Gualtieri[1] & C.M. Casciola[1]**

[1] Dipartimento di Ingegneria Meccanica e Aeronautica, "La Sapienza" University of Rome, Italy

[2] Linnè Flow Centre, KTH Royal Institute of Technology, Stockholm, Sweden

E-mail: `francesco.picano@uniroma1.it`

**Abstract.** DNS data of particle-laden jets are discussed both in the one- and two-way coupling regimes. Dynamics of inertial particles in turbulent jets is characterized by an anomalous transport that leads to the formation of particle concentration peaks along the jet axis. Larger is the particle inertia farther the peak location occurs. The controlling parameter is found to be the local large-scale Stokes number which decreases quadratically with the axial distance and is order one in coincidence of the peaks. The centerline mean particle velocity is characterized by two scaling laws. The former occurs upstream the location where the Stokes number is order one, and is linear in the axial distance with negative coefficient. The latter, occurring downstream where the local Stokes number is small, coincides with that of the centerline mean fluid velocity. This behavior affects the development of the particle-laden jet when the mass load of the particulate phase increases and two-way coupling effects become relevant. Two distinct behaviors for the jet development are found behind and beyond the location of unity local Stokes number leading to different scaling laws for the mean centerline fluid velocity.

## 1. Introduction

Particulate turbulent jets are frequently found in earth science (e.g. volcano eruption Kaminski *et al.*, 2005), physics (e.g. cloud dynamics Govindarajan, 2002) and engineering (e.g. sprays Sirignano, 1983). Two main phenomenologies affect the dynamics of turbulent jets: the entrainment process and the slight inhomogeneity in the streamwise direction. The former crucially determines the condition for the collapse of the two-phase jet-column that is at the origin of pyroclastic flows in volcano eruptions (Kaminski *et al.*, 2005). The gentle inhomogeneity in the axial direction associated to the mean centerline velocity decay influences the properties of the jet/spray penetration which is essential for combustion chambers of direct injection internal combustion engines (Sirignano, 1983; Siebers, 1999)

The inertial particle dynamics has been addressed in several turbulent flow configurations, e.g. homogeneous flows, pipe and channel flows, see Toschi & Bodenschatz (2009); Balachandar & Eaton (2010) for recent reviews. Peculiar transport properties are found to occur, e.g. small-scale clustering (Balkovsky *et al.*, 2001; Bec *et al.*, 2007; Gualtieri *et al.*, 2009; Coleman & Vassilicos, 2009) which consists of an intermittent particle spatial distribution composed of void regions and particle clusters. In wall bounded flows, a mean drift of the particles towards the wall is found, the so-called turbophoresis (Reeks, 1983; Rouson & Eaton, 2001; Marchioli *et al.*, 2008; Picano *et al.*, 2009). Several papers investigate the transport of inertial particles (e.g. Fan *et al.*, 2004; Longmire & Eaton, 1992)) or evaporating droplets (e.g. Almeida & Jaberi, 2006; Selle & Bellan, 2007)) in the near field region of jets. In this non-universal region, inertial particles are found to concentrate in the shear-layer outside the large coherent vortical structures which populate the near field, consistently with the general trend observed in other flows. Concerning the far field behavior, peak of mean particle concentration are observed on the axis. These humps are found to occur when the large-scale axial-dependent Stokes number is order one, (e.g. Picano *et al.*, 2010; Casciola *et al.*, 2010). A number of experimental works (e.g. Hardalupas *et al.*, 1989; Longmire & Eaton, 1992; Prevost *et al.*, 1996) investigate the back-reaction of the particles on the carrier fluid in the far field, where the jet is observed to decay at slower rate. Recently, semi-empirical fits on the scaling of the jet mean velocity are proposed in Foreman & Nathan (2009) as a function of the particle inertia and the overall mass load.

Purpose of the present contribution is to examine the dynamics of inertial particles in the one-way coupling regime and the effect of the particle back-reaction on the fluid stream in the two-way coupling regime using data from Direct Numerical Simulations of free particle-laden turbulent jets. As it will be shown, the one-way coupled dynamics of inertial particles in the jet far field is characterized by centerline concentration peaks and two different particle velocity scaling laws. This behavior crucially affects the flow dynamics when the mass load increases and two-way coupling effects become relevant. Actually the far field appears divided in two regions with different scaling laws for the mean centerline fluid velocity.

## 2. Numerical algorithm

The fluid phase algorithm is based on an explicit second-order staggered finite-difference scheme in conservative formulation. The cylindrical formulation of the incompressible Navier-Stokes equations are evolved in time by a low-storage third order Runge-Kutta scheme, (see Picano & Casciola, 2007; Picano *et al.*, 2009, 2011, for details on numerics and tests).

The jet is generated by a turbulent inflow that uses data from a companion DNS of a fully developed pipe flow with bulk Reynolds number $Re_R = U_0\,R/\nu = 2000$, where $R$ is the pipe radius, $U_0$ the bulk velocity and $\nu$ the kinematic viscosity. A typical run involves $784\times145\times128$ grid points in axial $z$, radial $r$, and azimuthal $\theta$ directions, respectively. Traction-free conditions are enforced on the side boundary at $r = 28\,R$, while convective outflow conditions are placed at $z = 83\,R$. The particles are assumed to be rigid and spherical with a diameter $d_p$ much smaller than Kolmogorov scale and with density much larger than the fluid one. As anticipated, we confine our analysis to the one-way and two-way coupling regimes considering sufficiently diluted suspensions to neglect inter-particle interactions (four-way coupling). In such conditions the only significant force acting on the particles is the viscous Stokes drag, and each particle evolves according to the simplified equations

$$\dot{\mathbf{v}} = (\mathbf{u}|_{\mathbf{p}} - \mathbf{v})/\tau_{\mathbf{p}} \qquad \dot{\mathbf{x}} = \mathbf{v}, \tag{1}$$

where $\mathbf{v}$ and $\mathbf{u}|_{\mathbf{p}}$ denote the particle velocity and the fluid velocity at particle position, while $\tau_p = \rho_p\,d_p^2/(\rho\nu 18)$ is the particle response time (Stokes time). A mixed linear-quadratic formula based on Lagrange polynomials is used to interpolate the fluid velocity at particle positions, see Picano *et al.* (2009, 2010). The back-reaction of the particles on the fluid is calculated by using the same formulas.

For a given jet, two parameters control the dynamics, the nominal Stokes number $St_0 = \tau_p U_0/R$ and the mass load ratio $\Phi = \dot{M}_p/\dot{M}_f$, defined as ratio of particle to fluid mass fluxes at the inflow. Concerning the very dilute limit (one-way coupling regime, $\Phi = 0$), six particle populations are considered differing for the Stokes number $St_0$, ranging from $St_0 = 4$ to $St_0 = 128$. The effect of the particle back-reaction is analyzed for two mass load ratios $\Phi = 0.38$

and $\Phi = 0.8$ and two different Stokes numbers $St_0 = 8$ and $St_0 = 16$. The injection rate is fixed at 1800 particles per eddy turnover time $T_0 = R/U_0$ for each simulation (the mass load ratio is changed by varying $\rho_p/\rho$).

## 3. Results and Discussions

### *3.1. One-way coupling regime,* $\Phi = 0$

A visual impression of the overall behavior of the turbulent jet with no particle back-reaction can be gained by observing the instantaneous iso-levels of the concentration of a passive scalar transported by the turbulent flow, figure 1. The instantaneous configurations of three particle populations (one-way coupling regime, $\Phi = 0$), namely $St_0 = 4$, $St_0 = 16$ and $St_0 = 128$, are superimposed on the passive scalar field in panels (a), (b) and (c) of figure 1, respectively. The smallest particles here considered exhibit an apparent small-scale clustering, e.g. Bec *et al.* (2007). On the contrary, the heaviest particles, $St_0 = 128$, show an almost even distribution in the whole field. Peculiarly, particles with $St_0 = 16$ presents both behaviors exhibiting an even arrangement up to the location denoted by the arrow and small-scale clustering beyond this point. This phenomenology may be explained considering that all the typical time-scales of the jet increase with the distance from the origin $z$. To properly describe the particle dynamics a local Stokes number should be based on the local time scale of the jet defined in terms of the characteristic velocity and length scale of the flow. Considering the large-scale behavior, the typical velocity of the jet is the mean centerline velocity:

$$U_c = A\frac{\sqrt{\dot{Q}}}{z - z_0} \tag{2}$$

where $\dot{Q}$ is the momentum flux of the jet that is a conserved quantity with $A$ a constant, (see Hussein *et al.*, 1994; Picano & Casciola, 2007, for more details). Equation (2) is usually expressed

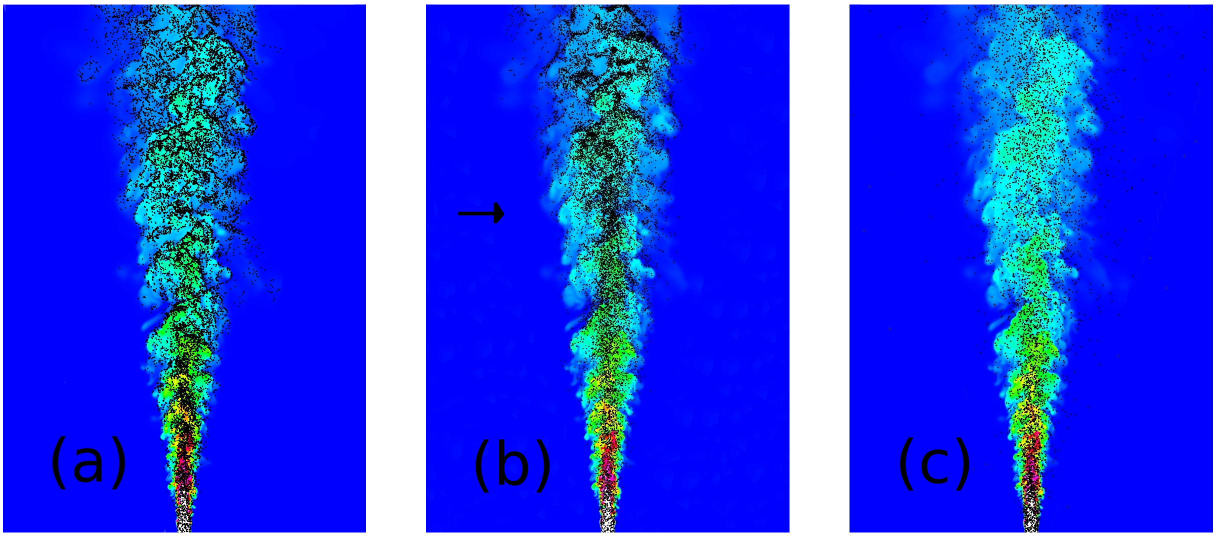


**Figure 1.** Instantaneous configuration of a thin axial-radial slice of the turbulent jet with $\Phi = 0$. Contours represent axial velocity intensities, dots represent the particle positions: (a) particles with $St_0 = 4$; (b) particles with $St_0 = 16$; (c) particles with $St_0 = 128$.

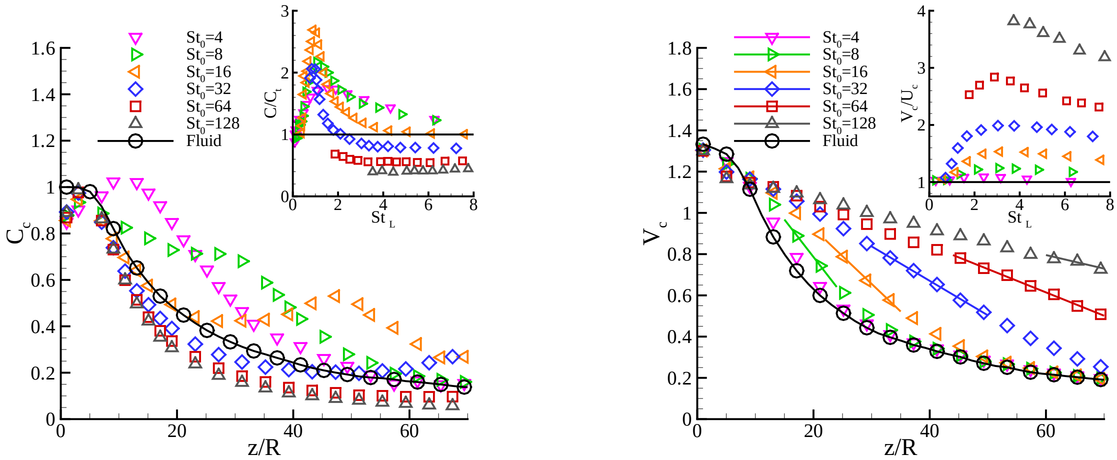


**Figure 2.** One-way coupling regime. Left panel, mean centerline concentration of particles and of a passive scalar (Smidth number $Sc = 0.7$) vs $z/R$; in the inset, the mean particle concentration normalized by the passive scalar concentration is plotted vs $St_L(z)$. Right panel, mean centerline velocity of particles and fluid vs $z/R$; in the inset the mean centerline particle velocity normalized by the mean centerline fluid velocity is plotted vs $St_L(z)$.

in terms of inlet bulk velocity $U_0$ and jet nozzle radius $R$:

$$U_c = B \frac{2R\,U_0}{z - z_0} \tag{3}$$

with

$$B = A \frac{\sqrt{\dot{Q}}}{2R\,U_0} \tag{4}$$

the decay constant of the jet. The typical large-scale length is the jet half-width (the radial distance where the mean velocity is half its centerline value) $r_{1/2} = S\,(z - z_0)$. The decay constant $B$ and the spreading rate $S$ are two almost universal constants which display a scatter of the order of 10% among different experiments and numerics (in this case $S = 0.089$, $B = 6.77$ $z_0 = -0.8\,R$, see George (1989); Hussein *et al.* (1994); Picano & Casciola (2007) for related discussions). The typical timescale of the flow is promptly defined as $T_L = r_{1/2}/U_c \propto z^2$ and the local large-scale Stokes number is,

$$St_L = \tau_p/T_L = \frac{\tau_p U_c}{r_{1/2}} = \frac{2\,B}{S} \left( \frac{R}{z - z_0} \right)^2 St_0. \tag{5}$$

As a consequence, the local Stokes number decreases quadratically with the distance from the origin: $St_L \propto (z - z_0)^{-2}$. Hence particles with different inertia assume the same values of $St_L$ at appropriate different distances from the origin. Actually the small-scale particle dynamics is controlled by the Kolmogorov based Stokes number that follows the same axial dependence being proportional to $St_L$, (Casciola *et al.*, 2010). In fact, particles with $St_0 = 16$ close to the jet inlet behave as very massive particles to become progressively *lighter* with increasing distance.

The left panel of figure 2 provides the axial behavior of the centerline mean particle concentration and of the passive scalar field for the jet in the one-way coupling regime. Particle populations show concentration peaks that move downstream increasing the inertia, namely $St_0$.

The location of these peaks is controlled by the local Stokes number $St_L$, as can be appreciated in the inset of the same figure where the normalized concentration is plotted as a function of $St_L$. Peaks occur at locations where $St_L = \mathcal{O}(1)$. Beyond this point particles tend to behave like tracers, $St_L \ll 1$, showing a centerline concentration close to that of a passive scalar.

The right panel of figure 2 provides the axial behavior of the centerline mean particle and fluid velocity for the one-way coupled jet. As for the particle concentration, the particle mean velocity is again controlled by $St_L$. The mean particle velocity collapses on the fluid one at growing distance for increasing $St_0$. In particular, as can be appreciated by the inset where the normalized particle velocity $V_c/U_c$ is plotted against $St_L$, when $St_L(z) < 0.7$ all the particles start to behave as tracers with $V_c/U_c \simeq 1$. Hence downstream the axial location where $St_L(z) = 0.7$ the mean particle centerline velocity assumes the scaling of the fluid mean centerline velocity $V_c \simeq U_c = U_0\, B\, 2R/(z - z_0)$. Before behaving as tracers, particles exhibit a mean centerline velocity that appears proportional to $z$ with a negative proportionality constant $K < 0$: $V_c \propto K\, z$, a feature particularly evident for particles with large $St_0$, figure 2. Actually, this behavior is common for all particle populations in a range of axial distances $z$ characterized by a local Stokes number in the interval: $St_L(z) \simeq 2 \div 5$. An explanation of this peculiar law can be derived considering the averaged Eulerian form of the particle dynamical equation (1) restricted to the jet axis (see Young & Leeming, 1997; Picano *et al.*, 2010, for more details):

$$V_c \frac{dV_c}{dz} + \overline{\mathbf{v}' \cdot \nabla v'_z} = \frac{U_c - V_c}{\tau_p}. \tag{6}$$

Roughly neglecting the second order terms $\overline{\mathbf{v}' \cdot \nabla v'_z}$, see Picano *et al.* (2010), and normalizing equation (6) by $V_c\, U_0/R$ we obtain:

$$\frac{dV_c}{dz}\frac{R}{U_0} = \frac{U_c/V_c - 1}{St_0}. \tag{7}$$

As can be observed in the inset of the right panel of figure 2, when $St_L \simeq 3$ the ratio $V_c/U_c$ assumes its maximum value greater than 1. Because in the range $St_L = 2 \div 5$ $V_c/U_c$ displays a small variation around its maximum, its value can be well approximated by the maximum itself $(V_c/U_c)|_{max}$ leading to a constant derivative for the mean particle centerline velocity:

$$\frac{dV_c}{dz}\frac{R}{U_0} = \frac{(U_c/V_c)|_{max} - 1}{St_0} = K < 0 \tag{8}$$

with $K$ negative. Figure 3 reports the values of $K$ vs $St_0$ estimated by fitting the data for each particle population in the range of axial distances where $St_L(z) = 2 \div 5$ (red symbols $+$); the range of axial distances considered for the fitting is reported by straight lines in the right panel of figure 2. These data are compared with the estimate given by equation (8), $K_e = [(U_c/V_c)|_{max} - 1]/St_0$ (green symbols $\times$). The agreement between estimated $K_e$ and the measured $K$ is excellent indirectly confirming the validity of the assumptions used to derive equation (8). As discussed in Picano *et al.* (2010) the value of the maximum $(U_c/V_c)|_{max}$ depends on $St_0$ in a non trivial way via a memory of the non-universal near field dynamics. This implies that $K$ does not scale with $St_0^{-1}$ as apparent at first sight from equation (8), see the blue dotted line in figure 3. Nonetheless, the scaling law $K \propto St_0^{-0.66}$ appears to well capture the dependence of $K$ on the nominal Stokes number $St_0$. Only particles with $St_0 = 8$ present a small displacement from the proposed scaling law, however it should be considered that for these particles the axial range where $St_L = 2 \div 5$ lies between $15 < z/R < 23$ a region where the far-field behavior of the fluid phase is still not fully established.

The two scaling laws found for the particle mean centerline velocity may reflect in different behaviors for the fluid mean velocity in case the mass load ratio increases and two-way coupling regime sets in.

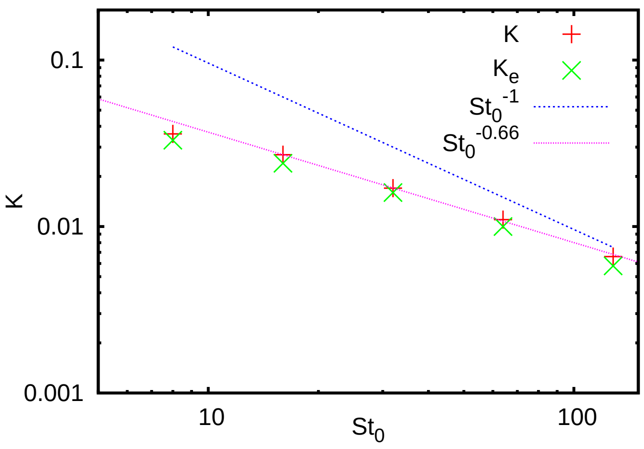


**Figure 3.** Opposite value of the constant $K$ vs $St_0$. The red symbols + represent $K$ obtained by fitting the data in the range of axial distances where $St_L(z) = 2 \div 5$. The green symbols $\times$ display $K_e$ estimated by the equation (8), $K_e = [(U_c/V_c)|_{max} - 1]/St_0$. The blue dotted line represents the scaling $K \propto St_0^{-1}$, the purple dashed line the scaling $K \propto St_0^{-0.66}$.

*3.2. Two-way coupling regime, $\Phi > 0$*

The behavior of the two-way coupling particle-laden jet at very large distance from the origin can be argued considering some results of the one-way coupling regime, at least for moderate mass loads. As discussed in the previous paragraph, at sufficient distance from the origin, $z/R \gg 1$, and despite their initial inertia, all inertial particles behave as tracers where the local Stokes number becomes negligible $St_L(z) \ll 1$. Data from the one-way coupling regime shows that equilibrium between the two phases is reached downstream the location where $St_L(z) = 0.7$ with the mean particle velocity matching the fluid one (see also Prevost *et al.*, 1996; Picano *et al.*, 2010). In this *extreme far field* the particulate flow can be considered as a single-phase flow with density variations related to the particle concentration. In this regime, the scaling of the mean centerline velocity should be similar to that of variable-density jets (e.g. Richards & Pitts, 1993). In particular, in equation (2) the momentum flux should take into account both phases: $\dot{Q} = \dot{Q}_f + \dot{Q}_p$, with $\dot{Q}_f$ and $\dot{Q}_p$ the momentum flux of the fluid and particulate phases, respectively. Since in present simulations the particles are injected at the inlet with the same local fluid velocity, the mass load ratio coincides with the momentum flux ratio $\Phi = \dot{M}_p/\dot{M}_f = \dot{Q}_p/\dot{Q}_f$ leading to

$$Q = Q_f + Q_p = (1 + \Phi)Q_f. \tag{9}$$

**Table 1.** Decay constants obtained fitting the data in the intermediate far field ($2 < St_L < 5$) $B_1$ and in the very far field ($St_L < 0.7$) $B_2$

| Case | $B_1$ | $B_2$ | $B\sqrt{1+\Phi}$ |
|---|---|---|---|
| $St_0 = 8,\ \Phi = 0.38$ | 10.8 | 8.5 | 8.0 |
| $St_0 = 16,\ \Phi = 0.38$ | 10.1 | 8.5 | 8.0 |
| $St_0 = 8,\ \Phi = 0.8$ | 17.8 | 9.5 | 9.1 |
| $St_0 = 16,\ \Phi = 0.8$ | 13.5 | 8.9 | 9.1 |

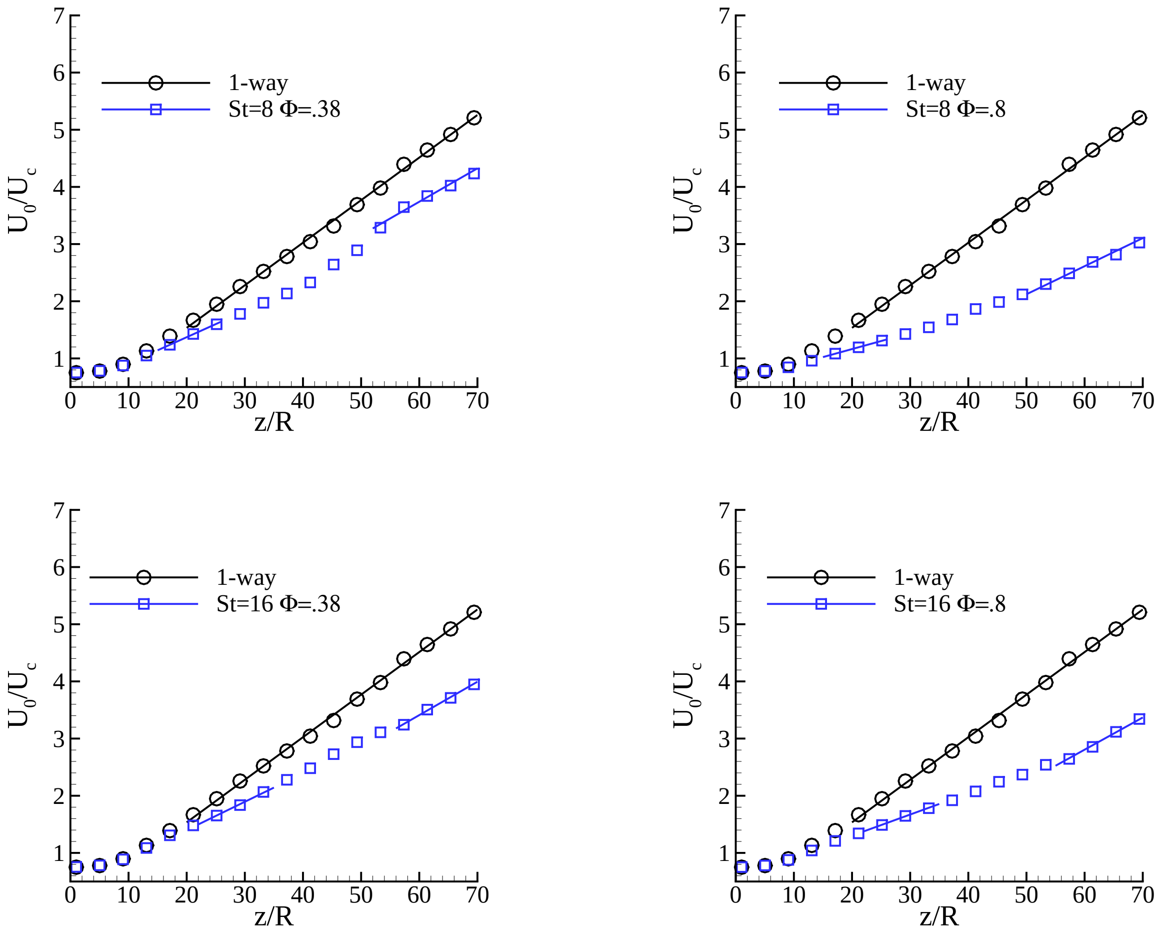


**Figure 4.** Mean centerline velocity of the fluid phase in the two-way coupling regimes for two different $St_0$ and $\Phi$. Black circles represent the unladen case (1-way), blue squares the 2-way coupling data. The straight lines denote linear fits of the data and extend only in the region where data are fitted. Top-left panel: $St_0 = 8$, $\Phi = 0.38$; top-right panel: $St_0 = 8$, $\Phi = 0.8$; bottom-left panel $St_0 = 16$, $\Phi = 0.38$; bottom-right panel: $St_0 = 16$, $\Phi = 0.8$.

Combining equations (2), (9), (4) it results:

$$U_c = B\sqrt{1+\Phi}\,\frac{2RU_0}{z-z_0}. \tag{10}$$

Hence the actual decay constant at sufficient distance from the origin, $St_L(z) < 0.7$, should increase from the original value $B$ to $B\sqrt{1+\Phi}$.

Before this ultimate regime is reached, the momentum exchange between the two phases determines a different scaling law for the centerline mean fluid velocity. Recalling that, in the one-way coupling regime, a scaling law for the mean particle velocity is found when $2 < St_L(z) < 5$, we expect that a corresponding scaling law for the mean centerline fluid velocity should exist also for the two-way particle-laden jet, at least for moderately large $\Phi$. However, given the remarkable memory effect of the particle dynamics (Picano *et al.*, 2010), a non trivial dependence on both $St_0$ and near field details could emerge.

Figure 4 shows the inverse of the mean centerline fluid velocity $U_c$ vs $z/R$ for four different

DNS of 2-way particle-laden jets with two mass load ratios, $\Phi = 0.38$ and $\Phi = 0.8$, and two nominal Stokes numbers, $St_0 = 8$ and $St_0 = 16$. As expected, the fluid centerline velocity decays at slower rate due to the forcing from the particulate phase. The decay constants $B_2$ of the mean centerline velocity in the extreme far field ($St_L < 0.7$) are extracted by fitting the data from the location where $St_L(z) = 0.7$ (the straight lines in the figure represent the corresponding fitting intervals) and reported in table 1. The differences between the estimated values $B\sqrt{1+\Phi}$ and the fitted ones $B_2$ is smaller than 10%. It should be remarked that, due to variations in the inflow details, the decay constant $B$ of unladen turbulent jets show a scatter of the order of 10% among experiments and DNSs (see George, 1989; Picano & Casciola, 2007). In addition, at least in the near field, a 2-way coupled particle-laden jet is affected by a strong turbulence modulation that alters the initial jet dynamics and may imprint the successive behavior of the jet, (George, 1989). Hence considering a two-way coupled particle-laden jet in the extreme far field, $St_L(z) < 0.7$, as a single-phase variable-density jet with a decay constant $B_2 = B\sqrt{1+\Phi}$ seems a fair approximation.

The intermediate far field appears to be characterized also by a linear scaling law for the inverse of the fluid centerline mean velocity, now with a different decay constant, $B_1$. Its value is here estimated by fitting the data in the region where $2 < St_L(z) < 5$, although the axial interval where the scaling law appears to hold seems wider. $B_1$, table 1, displays a clear dependence on both parameters $\Phi$ and $St_0$. Beyond giving evidence of the existence of a scaling law of the form $U_c = B_1 2RU_0/(z-z_0)$ in this intermediate far field, the present dataset does not allow a complete determination of its dependence on $St_0$ and $\Phi$. A more complete analysis is currently in progress to address this complicate issue.

## 4. Final remarks

DNS data on one-way and two-way coupling regimes of particle-laden jets have been presented. Concerning the one-way coupling regime, mean particle concentration peaks are found on the jet centerline. The peak location moves downstream when the particle inertia ($St_0$) increases. This phenomenology is controlled by a local large-scale Stokes number $St_L(z)$ which decreases quadratically with the axial distance. The peaks occur when $St_L \simeq 1$. Analogously, the mean particle velocity is mainly governed by $St_L(z)$. Mean particle velocity is usually larger than that of the fluid up to the location where $St_L(z) = 0.7$. In this intermediate far field, characterized by $2 < St_L(z) < 5$, a scaling law is found from theoretical arguments and confirmed by the data. In particular, the mean centerline particle velocity is found to be linear with a negative proportionality constant $K$, $V_c \propto K\,z$. The constant $K$ is found to scale with $St_0^{-0.66}$. Downstream the location where $St_L(z) = 0.7$, the mean particle velocity collapses on the fluid one.

These two distinct behaviors appear to reflect on the scaling of the fluid phase when the mass load ratio increases and two-way coupling conditions take place. In the very far field, $St_L(z) < 0.7$ the particle-laden jet can be considered as a single-phase variable-density jet. Consistently the decay constant of the mean centerline fluid velocity becomes $B_2 = B\sqrt{1+\Phi}$. In the intermediate far field, $2 < St_L(z) < 5$, the existence of a scaling law of the form $U_c = B_1\,2RU_0/(z-z_0)$ emerges from the data. However now the constant $B_1$ seems to depend in a non-trivial way on the particle inertia–$St_0$–and on the mass load ratio–$\Phi$. Further work is planned to better assess this issue.

## 5. Acknowledgments

Authors would thank the COST Action MP0806 Particles in Turbulence for supporting the present work and the CASPUR consortium where the simulations were performed.

## References

Almeida, T.G. & Jaberi, F.A. 2006 Direct numerical simulations of a planar jet laden with evaporating droplets. *International Journal of Heat and Mass Transfer* **49** (13-14), 2113.

Balachandar, S & Eaton, JK 2010 Turbulent Dispersed Multiphase Flow. *Annual Rev. Fluid Mech.* **42**, 111.

Balkovsky, E., Falkovich, G. & Fouxon, A. 2001 Intermittent distribution of inertial particles in turbulent flows. *Phys. Rev. Lett.* **86** (13), 2790–2793.

Bec, J., Biferale, L., Cencini, M., Lanotte, A., Musacchio, S. & Toschi, F. 2007 Heavy particle concentration in turbulence at dissipative and inertial scales. *Phys. Rev. Lett.* **98** (8), 084502.

Casciola, CM, Gualtieri, P, Picano, F, Sardina, G & Troiani, G 2010 Dynamics of inertial particles in free jets. *Physica Scripta* **T142**, 014001.

Coleman, SW & Vassilicos, JC 2009 A unified sweep-stick mechanism to explain particle clustering in two-and three-dimensional homogeneous, isotropic turbulence. *Phys. Fluids* **21**, 113301.

Fan, J., Luo, K., Ha, M.Y. & Cen, K. 2004 Direct numerical simulation of a near-field particle-laden plane turbulent jet. *Phys. Rev. E* **70** (2), 26303.

Foreman, RJ & Nathan, GJ 2009 Scaling of the gas phase in particle-laden turbulent axisymmetric jets. *International Journal of Multiphase Flow* **35** (1), 96.

George, W.K. 1989 Self-preservation of turbulent flows and its relation to initial conditions and turbulent structures. In *Advances in Turbulence*, p. 39. New York: Hemisphere.

Govindarajan, R. 2002 Universal behavior of entrainment due to coherent structures in turbulent shear flow. *Phys. Rev. Lett.* **88** (13), 134503.

Gualtieri, P., Picano, F. & Casciola, CM 2009 Anisotropic clustering of inertial particles in homogeneous shear flow. *J. Fluid Mech.* **629**, 25.

Hardalupas, Y., Taylor, A. & Whitelaw, JH 1989 Velocity and Particle-Flux Characteristics of Turbulent Particle-Laden Jets. *Proc. R. Soc. London A* **426** (1870), 31.

Hussein, H. J., Capp, S. P. & George, W. K. 1994 Velocity measurements in a high-Reynolds-number momentum-conserving, axisymmetric turbulent jet. *J. Fluid Mech.* **258**, 31.

Kaminski, E., Tait, S. & Carazzo, G. 2005 Turbulent entrainment in jets with arbitrary buoyancy. *J. Fluid Mech.* **526**, 361.

Longmire, E. & Eaton, J. 1992 Structure of a particle-laden round jet. *J. Fluid Mech.* **236**, 217.

Marchioli, C., Soldati, A., Kuerten, JGM, Arcen, B., Taniere, A., Goldensoph, G., Squires, KD, Cargnelutti, MF & Portela, LM 2008 Statistics of particle dispersion in Direct Numerical Simulations of wall-bounded turbulence: results of an international collaborative benchmark test. *International Journal of Multiphase Flow* **34** (9), 879.

Picano, F., Battista, F., Troiani, G. & Casciola, C. 2011 Dynamics of piv seeding particles in turbulent premixed flames. *Experiments in Fluids* **50**, 75–88.

Picano, F. & Casciola, CM 2007 Small-scale isotropy and universality of axisymmetric jets. *Phys. Fluids* **19**, 118106.

Picano, F., Sardina, G. & Casciola, C.M. 2009 Spatial development of particle-laden turbulent pipe flow. *Phys. Fluids* **21**, 093305.

Picano, F., Sardina, G., Gualtieri, P. & Casciola, CM 2010 Anomalous memory effects on transport of inertial particles in turbulent jets. *Phys. Fluids* **22**, 051705.

Prevost, F., Boree, J., Nuglisch, HJ & Charnay, G. 1996 Measurements of fluid/particle correlated motion in the far field of an axisymmetric jet. *Int. J. Multiphase Flow* **22** (4), 685.

Reeks, MW 1983 The transport of discrete particles in inhomogeneous turbulence. *J. of Aerosol Science* **14** (6), 729.

Richards, CD & Pitts, WM 1993 Global density effects on the self-preservation behaviour of turbulent free jets. *J. Fluid Mech.* **254**, 417–435.

Rouson, D.W.I. & Eaton, J.K. 2001 On the preferential concentration of solid particles in turbulent channel flow. *J. Fluid Mech.* **428**, 149.

Selle, LC & Bellan, J. 2007 Characteristics of transitional multicomponent gaseous and drop-laden mixing layers from direct numerical simulation: Composition effects. *Phys. Fluids* **19**, 063301.

Siebers, D.L. 1999 Scaling liquid-phase fuel penetration in diesel sprays based on mixing-limited vaporization. *SAE technical paper* pp. 01–0528.

Sirignano, William A. 1983 Fuel droplet vaporization and spray combustion theory. *Progress in Energy and Combustion Science* **9** (4), 291 – 322.

Toschi, F. & Bodenschatz, E. 2009 Lagrangian properties of particles in turbulence. *Annual Rev. Fluid Mech.* **41**, 375.

Young, J. & Leeming, A. 1997 A theory of particle deposition in turbulent pipe flow. *J. Fluid Mech.* **340**, 129.